1 **INFLUENCE OF ACTIVATION ATMOSPHERE USED IN THE CHEMICAL**

2 **ACTIVATION OF ALMOND SHELL ON THE CHARACTERISTICS AND**

3 **ADSORPTION PERFORMANCE OF ACTIVATED CARBONS**

4

5 Alicia Martínez de Yuso[1*], Begoña Rubio[2], M. Teresa Izquierdo[2]

6

7 [1] University of San Jorge, Autovía A23 Zaragoza-Huesca, km 510, 50830 Villanueva de

8 Gállego, Zaragoza, Spain

9 [2] Instituto de Carboquímica, ICB-CSIC, C/Miguel Luesma 4, 50018 Zaragoza, Spain

10

11 *corresponding author

12 e-mail: acmartinez@usj.es

13 voice: +34976060100

14 address: Campus Universitario Villanueva de Gállego. Autovia A-23 Zagaroza-Huesca

15 Km. 299. 50830 Villanueva de Gállego, Zaragoza (Spain).

16

17

18

19

20

21

22

23

24

25

ABSTRACT

The aim of this work was to compare the effect of different activating atmospheres on the final properties and adsorption performance of activated carbons. Almond shell based activated carbons have been obtained by chemical activation with phosphoric acid. Two sets of activated carbons were prepared. First set was prepared under inert atmosphere at different impregnation ratios, temperatures and times of activation. Second set of activated carbons was prepared at the same activating conditions except the activating atmosphere using and oxidant one. Activated carbons prepared under both activation atmospheres were characterized by elemental analysis (EA), thermogravimetry (TGA), temperature programed desorption (TPD), point zero charge (PZC), Boehm titration and N_2 physisorption. To study the adsorption performance of the activated carbons toluene adsorption-desorption isotherms were determined gravimetrically. The results obtained confirm that the activating atmosphere has a strong influence on the final characteristics of the activated carbons. Activated carbons with higher oxygen content and more negative surface charge have been obtained by changing the activating atmosphere by an oxidant one. Surface area is also higher for activated carbons prepared under oxidant atmosphere. However toluene adsorption capacity is lower for activated carbons prepared under oxidant atmosphere due to their surface chemistry.

KEYWORDS: activated carbons, activation atmosphere, chemical activation, adsorption, air pollution control, agricultural waste.

1. INTRODUCTION

Activated carbons are one of the most versatile adsorbents to be used for the effective removal of volatile organic compounds in gas streams [1]. The adsorption capacity of an activated carbon depends on the porosity [2,3], mainly on the microporosity, and on the surface chemistry [4].

Depending on the characteristics of the adsorbates, activated carbons can be designed by using the appropriate precursor and optimizing the preparation conditions, this is known as tailoring concept [5]. Main parameters affecting the characteristics of activated carbon are impregnation ratio, activation temperature, activation time and activating atmosphere.

Activated carbons can be produced from a large variety of raw materials by chemical or physical activation [6]. Advantages of the chemical activations compared to the physical activation are the lower activation temperature and the shorter activation time. The chemical activation involves the impregnation of the raw material with a chemical agent and the heat treatment of the mixture to carbonize the material. Different activated agents can be used in the chemical activation but phosphoric acid permits the preparation of activated carbons with lower activation temperatures [7,8]. Phosphoric acid promotes the depolymerization, dehydration and redistribution of constituent biopolymers [9] during the pyrolytic decomposition of lignocellulosic materials. Activated carbons with a large development of porosity can be prepared from lignocellulosic wastes by chemical activation with phosphoric acid [10-14].

The preparation of activated carbons by chemical activation with phosphoric acid under inert atmosphere, usually N_2, has been studied by several authors [8,11,15-17]. Although the effect of the phosphoric acid on the activation of activated carbons is well

76   defined, the effect of the atmosphere during the heat treatment has only been studied by

77   few authors [18-21].

78   Puziy et al. [12] obtained activated carbons with a higher oxygen content when an air

79   atmosphere is used instead of N_2 atmosphere. Porosity of activated carbons is also

80   affected by the activating atmosphere; the use of an oxidant atmosphere instead of an

81   inert atmosphere produce activated carbon with larger surface areas [12,19-22] and an

82   increase in mesopore volume [21,23] due to the widening of the pores during the

83   activation process. It can be explained in terms of the aromatization process during heat

84   treatment. The presence of oxygen inhibits the aromatization process, reducing the

85   influence of the phosphoric acid in both promoting the development of porosity and

86   reducing the extent of contraction produced during the heat treatment [18].

87   The present work compares the characteristics of activated carbons obtained by

88   chemical activation of almond shells as well as their toluene adsorption performance of

89   two series of activated carbons prepared with the same activation conditions except the

90   activating atmosphere: either under N_2 or $8\%O_2/N_2$ atmosphere.

91

92   **2. MATHERIAL AND METHODS**

93

94   2.1 Preparation of activated carbons

95

96   Raw material chosen for the preparation of activated carbons was almond shell from

97   Vera del Moncayo, Zaragoza (Spain). Dry shells were crushed and sieved at 0.2-1 mm.

98   The chemical activation was carried out by impregnation of the almond shell with

99   (ortho)-phosphoric acid of 89 wt. % followed by one-step carbonization-activation

100   under N_2 or in $8\%O_2/N_2$ atmosphere.

4

101 Impregnation ratio (defined as: weight of phosphoric acid / weight of precursor),

102 activation temperature and activation time were selected according to a previous work

103 [15]. In that work, a total of 12 activated carbons were prepared under N_2 atmosphere.

104 The activation conditions which led to activated carbons with higher toluene adsorption

105 capacities [24] were selected to prepare the new activated carbons under $8\%O_2/N_2$

106 activating atmosphere.

107 Before activation, the almond shell is mixed with a determined amount of phosphoric

108 acid of 89 wt % concentration to reach the impregnation ratios in the range 0.5-1.5. The

109 suspension was shaken at room temperature during 1 h. The impregnated samples were

110 further thermally treated at different activation temperatures under a flow of 250

111 cm^3/min either of $8\%O_2/N_2$ (which was kept during both heating and cooling), and

112 maintained at the selected temperature during a time ranging from 30 to 120 min. Solid

113 pyrolysis residues were water washed in Soxhlet until pH>6. The resulting activated

114 carbons were dried at 100ºC until constant weight and stored under Ar.

115 The activated carbons included in this study are given in Table 1.

116

117 2.2 Characterization of activated carbons

118

119 Activated carbons were characterized by elemental analysis, thermogravimetry (TGA)

120 temperature programmed desorption coupled to mass spectrometry (TPD-MS), point of

121 zero charge (PZC), Boehm titration and nitrogen adsorption at -196 ºC.

122 Ultimate analysis of the activated carbons was carried out in a Thermo Flash 1112

123 microanalysis apparatus. Oxygen content was obtained by difference.

124   Thermogravimetric (TG) curves were obtained in a TA Instruments thermobalance.

125   Approximately 20 mg of sample was placed in a Pt crucible and was heated at 10ºC/min

126   up to 1000ºC under a flow of Ar.

127   The TPD runs were carried out with a custom build set-up, consisting of a tubular

128   quartz reactor placed inside an electrical furnace connected to a quadrupole mass

129   spectrometer from Pfeifer. TPD experiments were carried out by heating the samples in

130   Ar flow up to 1100 ºC at a heating rate of 10 ºC/min, and recording the amount of CO

131   and CO_2 evolved at each temperature with the mass spectrometer. The calibrations for

132   CO and CO_2 were carried out by standards diluted in Ar. For each experiment 0.5 g of

133   activated carbon was placed in a horizontal quartz tube reactor under a stream of 30

134   ml/min of Ar.

135   The immersion technique [25] was used to determine the point of zero charge of the

136   samples. Suspensions of 0.7 g of activated carbon were put in contact with 10 ml of

137   $NaNO_3$ 0.1 M at different pH values. Initial pH values were obtained by adding an

138   amount of HNO_3 or NaOH solution taking the $NaNO_3$ solution to pH≈3, pH≈6 and

139   pH≈10. The suspensions were agitated for 24 h in a shaker at 250 r.p.m. at room

140   temperature and filtered. The pH of the filtered solutions were measured. The final

141   values for the PZC were the average of the three pH values.

142   The selective neutralization method was used to evaluate the acidic character of the

143   surface of the activated carbons according to Boehm's procedure [26]. The amounts of

144   various acidic oxygen functional groups (carboxyls, lactones, phenols and carbonyls)

145   were measured by selective neutralization using bases of different strength.

146   Approximately 0.5 g of each sample was mixed with 50 ml of a 0.1 N solution of a base

147   (NaOH, Na_2CO_3, $NaHCO_3$, $NaOC_2O_5$). The suspension was shaken for 24 h at room

148   temperature. After that time, the solution was filtered and an aliquot was taken. The

6

149   amount of each base neutralized by the activated carbon was determined by back-

150   titration using HCl 0.1 N solution.

151   The nitrogen adsorption at -196 ℃ was carried out in a Micromeritics ASAP 2020

152   automatic adsorption apparatus. The samples were initially outgassed at 150 ℃ and up

153   to a vacuum of 10^{-6} mm Hg. The volume of adsorbed nitrogen was measured from a

154   relative pressure of 10^{-7} up to 0.995. The isotherms were analysed using different

155   methods such as the BET method [27] for determination of surface area, the BJH

156   method [28] for determining the volume of mesopores and t-plot for determining the

157   volume of micropores [29]. The total pore volume was taken from the measurement of

158   adsorbed nitrogen at a relative pressure of 0.995.

159

160   2.3 Toluene adsorption

161

162   The adsorption-desorption isotherms of toluene were determined gravimetrically using

163   an automatic adsorption apparatus (VTI Co). The temperature of the sample, 25 ℃, was

164   monitored during the experiment and a pressure transducer monitored the pressure of

165   the system. For each experiment 80 mg of activated carbon was taken. Initially the

166   sample was outgassed at 150 ℃ and up to a vacuum of 10^{-6} mm Hg. After cooling to 25

167   ℃ toluene was introduced in the system to obtain the adsorption and desorption

168   isotherms.

169

170   **3. RESULTS AND DISCUSSION**

171

172   3.1 Characterization of samples

173

174 Elemental analysis and yield of activated carbons (calculated as 100 x mass of AC /

175 mass precursor) is included in Table 2. Activated carbons show a low content in

176 nitrogen and a negligible amount of sulfur. Activated carbons prepared under oxidant

177 atmosphere and at lower activation temperatures (400ºC) show a higher amount of

178 oxygen [12].

179 Activated carbons prepared at low and intermediate impregnation ratio show higher

180 yields [30,31]. It can be attributed to the decomposition of the polymeric structures of

181 the activated carbons during the activation stage that release most elements different

182 from carbon (N, H and O). Activating agent employed permits the dehydration,

183 depolimerization and the redistribution of the constituent polymers, and the conversion

184 of aliphatic groups to aromatics, increasing the yield of the activated carbons. Higher

185 impregnation ratios produce a higher elimination of tars of the pores decreasing the

186 yield [17].

187 Different activation atmospheres provided different yields [12], obtaining higher results

188 of yield for activated carbons prepared under oxidant atmosphere and low activation

189 temperatures. This can be attributed to the inhibition of the activating agent in presence

190 of air [18].

191 Figure 1 shows DTG curves for activated carbons obtained under inert and oxidant

192 atmospheres. Lignocellulosic wastes are mainly compound of hemicellulose, cellulose,

193 lignin and other polymers [32]. Hemicellulose decomposes at low temperatures (310 ºC)

194 while cellulose decomposes at higher temperature (at around 380 ºC) [33,34]. Lignin

195 starts to decompose at low temperature (220 ºC) and at low rate up to about 900 ºC

196 overlapping with the temperatures of decomposition of hemicellulose and cellulose

197 [35]. The addition of chemicals to the precursor and the thermal treatment carried out

198   result in a variation in the temperature of decomposition in function of the employed

199   conditions [33,36] shifting degradation to considerably higher temperatures [37].

200   The temperature used to prepare the activated carbons is higher than the decomposition

201   temperature of hemicellulose and cellulose therefore the curves of DTG obtained do not

202   present the processes corresponding to their decomposition, except for the activated

203   carbons AT400R15t30 and AT400R15t30-ox, due to the short time of activation

204   employed.

205   The activated carbons prepared at lower temperatures (400-467 ºC) present a broad

206   band around 550 ºC, which can indicate that the degradation process of the lignin has

207   been incomplete. The higher bands obtained for activated carbons prepared under

208   oxidant atmosphere indicate that this process has been more incomplete than for the

209   activated carbons prepared under inert atmosphere.

210   The band at about 800 ºC becomes more intense and it is shifted to higher temperatures

211   of decomposition at increasing temperature of activation. This band can indicate that the

212   crosslinking process to produce aromatic units becomes more important for activated

213   carbons prepared under inert atmosphere due to the higher bands obtained. The oxidant

214   atmosphere inhibits the production of aromatic units in the activation stage.

215   At the temperature of activation of 600ºC the crosslinking process has started during

216   activation of the samples and during TGA experiments this process is completed at

217   temperatures around 900 ºC.

218   During the thermal decomposition of activated carbons the surface oxygen complexes

219   are desorbed as CO and CO_2 at specific temperatures. It has been proposed that CO_2

220   evolves from carboxylic groups and their derivatives, such as lactones and anhydrides,

221   while CO is mainly a decomposition product of quinones, hydroxyquinones and phenols

222   [38,39].

223　Profiles of CO and CO_2 evolution are given elsewhere [40]. Since them, it can be

224　summarized that the preparation of activated carbons under oxidant atmosphere results

225　in the formation of more stable functional groups in the surface. These results can be

226　compared with the results obtained in DTG curves.

227　The amounts of CO and CO_2 evolved up to 1100ºC in TPD experiments are reported in

228　Table 3. For all samples studied the amount of CO evolved during the thermal treatment

229　is higher than the amount of CO_2. For activated carbons prepared under N_2 atmosphere,

230　increasing the activation temperature the amount of CO evolved increases but there is

231　no relationship with the amount of CO_2. Activated carbons prepared under oxidant

232　atmosphere show higher amounts of CO evolved than activated carbons prepared under

233　inert atmosphere, except for the activated carbons prepared at lower activation time

234　AT400R15t30-ox and AT600R1t30-ox. This result could be explained in terms of the

235　low activation time used. The aromatization process is inhibited under oxidant

236　atmosphere, as it has been shown above, but low activation times enhance this

237　inhibition.

238　The point of zero charge (PZC) is a very important parameter characterizing the acid-

239　base behaviour of the solids. In sorption studies is an useful parameter that permits to

240　hypothesise on the ionization of functional groups in the surface of activated carbons

241　and their interactions with adsorbates. PZC is defined as the value of pH at which the

242　charge of the solid surface is zero [41]. At this pH, the charge of the positive surface

243　sites is equal to that of the negative ones.

244　PZC of the activated carbons can be seen in Table 3. All samples have noticeably acid

245　properties with PZC values between 1.69 and 4.54. This can be explained by the

246　formation of acidic groups at the carbon surface as a result of the activating agent. It can

247　be observed that with the same preparation conditions activated carbons prepared under

10

248 oxidant atmosphere show a lower pH_{PZC}. It can be explained by the formation of a

249 higher amount of oxygenated surface groups on the activated carbons in presence of an

250 oxidant atmosphere. Both, under inert and in oxidant atmospheres, the value of pH_{PZC}

251 decreases at increasing the activation temperature.

252 Differences in the values of pH_{PZC} are a consequence of different preparation

253 conditions, confirming that, by carefully selecting the conditions of preparation, it is

254 possible to prepare activated carbons with different acidity levels and oxygen surface

255 groups distribution [42].

256 The selective base neutralization method gives information only on the oxygen surface

257 functionality of the carbons. Despite that not all the oxygen known to be on a carbon

258 surface can be measured by titration techniques, Boehm titration [26] was used to obtain

259 the amount of acidic sites on the activated carbon surface. Some oxygen could be

260 bonded within the graphene layers (in-ring) and hence would be non-reactive, and some

261 carbonyl groups may not be able to react with the alkaline solutions. Figure 2 reports

262 the results from Boehm titration. Main contribution to the surface chemistry

263 corresponds to carbonyls type groups, while the low content in phenolic groups respect

264 to the contribution of carbonyls groups has been described previously for activated

265 carbons from lignocellulosic materials activated with phosphoric acid [43]. Assuming

266 that carboxyls and lactones evolve CO_2 in TPD experiments and phenols and carbonyls

267 evolve as CO in TPD experiments, Boehm titration results follow the same trend

268 obtained from TPD experiments.

269 The characterization of porosity of samples obtained by the analysis of the N_2

270 physisorption is included in Table 4 and the isotherms obtained are shown in Figure 3.

271 The percentage of microporosity was obtained as the ratio between total micropore

272   volume, calculated applying the Dubinin-Radushkevich equation [44] to the adsorption

273   branch of the N_2 isotherm and the volume adsorbed at relative pressure of 0.995 [2].

274   For the activated carbons prepared under N_2 atmosphere, lower activation temperatures

275   (400-467 ºC), intermediate impregnation ratios (1.0-1.17) and intermediate activation

276   times (45-75 min) result in highest surface area BET. This is also confirmed taken into

277   account the values of micropore and mesopore volumes. This is in agreement with

278   others research works that prepare activated carbons from lignocellulosic wastes by

279   chemical activation with H_3PO_4 and obtain higher BET surface areas at activation

280   temperatures of 400-450 ºC [11,13,45] and with intermediate impregnation ratios

281   [10,46].

282   All activated carbons prepared under oxidant atmosphere show higher BET surface area

283   than those activated carbons prepared as same conditions under inert atmosphere. This

284   has been reported by other authors that obtain activated carbons with higher BET

285   surface area by changing an inert atmosphere by an oxidant one [12,16,21,22,47]. The

286   BET surface area of activated carbons prepared under oxidant atmosphere is a function

287   of the BET surface area of the activated carbons prepared under inert atmosphere [48].

288   The reproducibility of the preparation method used was tested previously [15], showing

289   a slightly variation, for example a difference of 1% in the BET surface area or 0.8% in

290   the carbon content.

291

292   3.2 Toluene adsorption

293

294   The static adsorption isotherms for toluene at 25 ºC are shown in Figure 4. The

295   experimental adsorption capacity, defined as the amount at the plateau of the isotherm,

296   is higher for the samples prepared at lower temperatures (400-467 ºC), for both inert

297 and oxidant atmosphere. Toluene adsorption capacities for activated carbons prepared

298 under inert atmosphere are slightly higher than for those activated carbons prepared at

299 the same activating conditions under oxidant atmosphere. This can be explained by the

300 higher amount of oxygenated groups present on the surface of activated carbons

301 prepared under oxidant atmosphere which have a negative influence on the toluene

302 adsorption capacity [14,49]. Samples with lower adsorption capacity are the samples

303 prepared at 533 ºC, which are the samples with the lower impregnation ratio, and the

304 sample prepared at 600 ºC. The adsorption capacities for each activated carbon are

305 included in Table 4.

306 Activated carbons show high toluene adsorption capacities, higher than 60% (wt/wt).

307 These values are higher than the adsorption capacities reported by other authors [4,50-

308 53].

309 The experimental adsorption isotherm data were fitted to the Langmuir model [54]. The

310 parameters of limiting value for toluene adsorption (W_m) and constant value (K)

311 obtained are resumed in Table 5. The Langmuir isotherm expressed relatively well the

312 adsorption of toluene, indicating the dependence on both physical and chemical

313 adsorption. W_m has a good correlation with the experimental results obtained for toluene

314 adsorption. Values of K can be related with the development of the microporosity of the

315 activated carbons.

316 Comparing the amount of toluene adsorbed with BET surface area it can be concluded

317 that there is not a direct correlation between both values. Activated carbons with higher

318 values of BET surface area do not show the higher adsorption capacities. In spite of

319 BET surface area is a very important parameter in toluene adsorption there are another

320 factors with a high influence on the toluene adsorption capacity. Surface chemistry is an

321 important characteristic of activated carbons which gives different adsorption sites.

322 From Table 3 and Figure 4, it is evident that the activated carbons have different

323 polarity coming from the different type and amount of surface groups. However,

324 comparing the amount of surface groups and toluene adsorption capacity it is clear that

325 there is not relationship. This fact can be explained in terms of a compromise between

326 textural properties and surface chemistry.

327 The heterogeneity of the activated carbon surface could give preferred sites for the

328 adsorption. This heterogeneity should be a compromise between adsorption potential

329 distribution in micropores and surface chemistry.

330 The heterogeneity of the surfaces can be studied by inspection of the deviation from

331 linearity of the D-R model applied to either n-hexane or toluene isotherms at high

332 relative pressures [55]. When a polar adsorbate is adsorbed onto a surface containing

333 polar sites there is a thermal effect on the orientation of the molecule on the adsorbent.

334 So the distribution of the adsorbed volumes with $-\Delta G$ for such a system should not

335 representative solely of the physical nature of the surface but will also be markedly

336 affected by its chemical nature.

337 Present case, all the toluene isotherms modeled by D-R equation exhibit a positive

338 deviation at the highest relative pressures (low $\log^2 p_0/p$).

339 At the lowest relative pressures, the adsorption capacities are strongly influenced by

340 electronic properties of the adsorbate and also with the energy of interaction with the

341 adsorbent. This fact is in line with adsorption capacities being associated with strong

342 interaction between adsorbent and adsorbate at the early stages of adsorption,

343 corresponding to primary micropore filling. During the later stages of adsorption, as

344 micropores of bigger size are being filled, at higher relative pressures, the adsorption

345 capacities are determined mainly by molecular size, the hydrophilic character of the

346 adsorbate and polarity. The importance of these properties indicates that polar as well as

14

347   non-polar interactions between adsorbate molecules play a key role in the adsorption

348   mechanism at this stage. At high relative pressures range the adsorption capacity is

349   affected by both mechanisms [55]. These positive deviations at high relative pressures

350   (low $\log^2 p_0/p$) from the D-R equation indicate that the adsorption process is dominated

351   by surface heterogeneity rather than volume filling of micropores.

352   The role played by both the chemical nature of the surface and the microporosity in the

353   deviation of the D-R plots may be quantified by calculating the slope of the portion of

354   the plot corresponding to high relative pressures (low $\log^2 p_0/p$) responsible of the

355   deviation from linearity.

356   The amount of toluene adsorbed is plotted as a function of the D-R slope at low $\log^2 p_0/p$

357   in Figure 5. It can be observed that there is a maximum of adsorption capacity at

358   intermediate values of D-R slope. This fact can indicate that there is a compromise

359   between porosity and surface chemistry, existing an optimum value to reach high

360   toluene adsorption capacity. High values for D-R slope deviation imply high surface

361   heterogeneity which can involve accessibility problems to the microporosity because

362   the high concentration of surface sites.

363   Low values for D-R slope deviation can imply lower concentration of adsorption sites,

364   leading to lower toluene adsorption characteristics.

365

366   **CONCLUSION**

367

368   The results of this study indicate that activating atmosphere during phosphoric acid

369   chemical activation of almond shell has a strong influence on the characteristics and

370   toluene adsorption capacity of the activated carbons. Activated carbons with higher

371   surface area can be obtained by changing an inert activating atmosphere by an air

372 atmosphere. The surface chemistry of activated carbons can be modified by using an

373 oxidant atmosphere, resulting in activated carbons with higher contents in oxygenated

374 surface groups and surface negative charge.

375 Toluene adsorption capacity is lower for activated carbons prepared under air

376 atmosphere in spite of their higher surface area. This can be attributed to the surface

377 chemistry of the activated carbons.

378 A compromise between textural properties and surface chemistry has been found in

379 terms of surface heterogeneity defined as the deviation of linearity of D-R plot,

380 obtaining maximum of adsorption capacity at intermediate values of D-R slope.

381

385

386 **References**

387 [1] L.K. Wang, N.C. Pereira, Y.T. Yung, Air pollution control engineering, in: K.H. Li

388   (Ed.), Handbook of Environment Engineering Volume I, Humana Press Inc.,

389   2004.

390 [2] M.A. Lillo-Rodenas, D. Cazorla-Amoros, A. Linares-Solano, Behaviour of

391   activated carbons with different pore size distributions and surface oxygen groups

392   for benzene and toluene adsorption at low concentrations, Carbon 43 (2005) 1758-

393   1767.

394 [3] A. Silvestre-Albero, J. Silvestre-Albero, A. Sepulveda-Escribano, F. Rodriguez-

395   Reinoso, Ethanol removal using activated carbon: Effect of porous structure and

396   surface chemistry, Microporous and Mesoporous Materials 120 (2009) 62-68.

397   [4]   K.J. Kim, C.S. Kang, Y.J. You, M.C. Chung, M.W. Woo, W.J. Jeong, N.C. Park,

398   H.G. Ahn, Adsorption-desorption characteristics of VOCs over impregnated

399   activated carbons, Catalysis Today 111 (2006) 223-228.

400   [5]   S.A. Dastgheib, D.A. Rockstraw, Pecan shell activated carbon: synthesis,

401   characterization, and application for the removal of copper from aqueous solution,

402   Carbon 39 (2001) 1849-1855.

403   [6]   H. Marsh, F. Rodríguez Reinoso, Activated Carbon, Elsevier Ltd, 2006.

404   [7]   A.M. Youssef, N.R.E. Radwan, I. Abdel-Gawad, G.A.A. Singer, Textural

405   properties of activated carbons from apricot stones, Colloids and Surfaces a-

406   Physicochemical and Engineering Aspects 252 (2005) 143-151.

407   [8]   M.J. Prauchner, F. Rodriguez-Reinoso, Preparation of granular activated carbons

408   for adsorption of natural gas, Microporous and Mesoporous Materials 109 (2008)

409   581-584.

410   [9]   M. Jagtoyen, F. Derbyshire, Activated carbons from yellow poplar and white oak

411   by H3PO4 activation, Carbon 36 (1998) 1085-1097.

412   [10] P. Patnukao, P. Pavasant, Activated carbon from Eucalyptus camaldulensis Dehn

413   bark using phosphoric acid activation, Bioresource Technology 99 (2008) 8540-

414   8543.

415   [11] B. Corcho-Corral, M. Olivares-Marin, C. Fernandez-Gonzalez, V. Gomez-Serrano,

416   A. Macias-Garcia, Preparation and textural characterisation of activated carbon

417   from vine shoots (Vitis vinifera) by H3PO4 - Chemical activation, Applied

418   Surface Science 252 (2006) 5961-5966.

419   [12] A.M. Puziy, O.I. Poddubnaya, A. Martinez-Alonso, A. Castro-Muniz, F. Suarez-

420   Garcia, J.M.D. Tascon, Oxygen and phosphorus enriched carbons from

421   lignocellulosic material, Carbon 45 (2007) 1941-1950.

422 [13] Y.P. Guo, D.A. Rockstraw, Activated carbons prepared from rice hull by one-step

423   phosphoric acid activation, Microporous and Mesoporous Materials 100 (2007)

424   12-19.

425 [14] R.R. Bansode, J.N. Losso, W.E. Marshall, R.M. Rao, R.J. Portier, Adsorption of

426   volatile organic compounds by pecan shell- and almond shell-based granular

427   activated carbons, Bioresource Technology 90 (2003) 175-184.

428 [15] M. Teresa Izquierdo, A. Martinez de Yuso, B. Rubio, M. Rosa Pino, Conversion of

429   almond, shell to activated carbons: Methodical study of the chemical activation

430   based on an experimental design and relationship with their characteristics,

431   Biomass & Bioenergy 35 (2011) 1235-1244.

432 [16] C.A. Toles, W.E. Marshall, M.M. Johns, Phosphoric acid activation of nutshells for

433   metals and organic remediation: Process optimization, Journal of Chemical

434   Technology and Biotechnology 72 (1998).

435 [17] N.M. Haimour, S. Emeish, Utilization of date stones for production of activated

436   carbon using phosphoric acid, Waste Management 26 (2006) 651-660.

437 [18] M. Molinasabio, F. Caturla, F. Rodriguezreinoso, Influence of the atmosphere used

438   in the carbonization of phosphoric-acid impregnated peach stones, Carbon 33

439   (1995).

440 [19] C.A. Toles, W.E. Marshall, M.M. Johns, Surface functional groups on acid-

441   activated nutshell carbons, Carbon 37 (1999).

442 [20] C. Moreno-Castilla, F. Carrasco-Marin, M.V. Lopez-Ramon, M.A. Alvarez-

443   Merino, Chemical and physical activation of olive-mill waste water to produce

444   activated carbons, Carbon 39 (2001).

445 [21] H. Benaddi, D. Legras, J.N. Rouzaud, F. Beguin, Influence of the atmosphere in

446   the chemical activation of wood by phosphoric acid, Carbon 36 (1998) 306-309.

447   [22] J. Laine, A. Calafat, M. Labady, Preparation and characterization of activated

448   carbons from coconut shell impregnated with phosphoric-acid, Carbon 27 (1989).

449   [23] Z.H. Hu, M.P. Srinivasan, Y.M. Ni, Preparation of mesoporous high-surface-area

450   activated carbon, Advanced Materials 12 (2000).

451   [24] M.T. Izquierdo, A.M. de Yuso, R. Valenciano, B. Rubio, M.R. Pino, Influence of

452   activated carbon characteristics on toluene and hexane adsorption: Application of

453   surface response methodology, Applied Surface Science 264 (2013) 335-343.

454   [25] B.M. Babic, S.K. Milonjic, M.J. Polovina, B.V. Kaludierovic, Point of zero charge

455   and intrinsic equilibrium constants of activated carbon cloth, Carbon 37 (1999)

456   477-481.

457   [26] H.P. Boehm, Some aspects of the surface chemistry of carbon clacks and other

458   carbons, Carbon, 1994, pp. 759-769.

459   [27] S. Brunauer, P.H. Emmett, E. Teller, Adsorption of gases in multimolecular layers,

460   Journal of the American Chemical Society 60 (1938) 309-319.

461   [28] E.P. Barrett, L.G. Joyner, P.P. Halenda, The determination of pore volume and area

462   distributions in porous substances .1. computations from nitrogen isotherms,

463   Journal of the American Chemical Society 73 (1951) 373-380.

464   [29] B.C. Lippens, J.H. Deboer, Studies on pore systems in catalysts .v. t method,

465   Journal of Catalysis 4 (1965) 319-&.

466   [30] D. Prahas, Y. Kartika, N. Indraswati, S. Ismadji, Activated carbon from jackfruit

467   peel waste by H3PO4 chemical activation: Pore structure and surface chemistry

468   characterization, Chemical Engineering Journal 140 (2008) 32-42.

469   [31] M. Molina-Sabio, F. Rodriguez-Reinoso, Role of chemical activation in the

470   development of carbon porosity, Colloids and Surfaces a-Physicochemical and

471   Engineering Aspects 241 (2004) 15-25.

472   [32] S. Balci, T. Dogu, H. Yucel, Pyrolysis kinetics of lignocellulosic materials,

473   Industrial & Engineering Chemistry Research 32 (1993) 2573-2579.

474   [33] R. Font, A. Marcilla, E. Verdu, J. Devesa, Thermogravimetric kinetic-study of the

475   pyrolysis of almond shells and almond shells impregnated with COCL2, Journal

476   of Analytical and Applied Pyrolysis 21 (1991) 249-264.

477   [34] J.A. Caballero, J.A. Conesa, R. Font, A. Marcilla, Pyrolysis kinetics of almond

478   shells and olive stones considering their organic fractions, Journal of Analytical

479   and Applied Pyrolysis 42 (1997) 159-175.

480   [35] J.F. Gonzalez, S. Roman, J.M. Encinar, G. Martinez, Pyrolysis of various biomass

481   residues and char utilization for the production of activated carbons, Journal of

482   Analytical and Applied Pyrolysis 85 (2009) 134-141.

483   [36] F. Suarez-Garcia, A. Martinez-Alonso, J.M.D. Tascon, Activated carbon fibers

484   from Nomex by chemical activation with phosphoric acid, Carbon 42 (2004)

485   1419-1426.

486   [37] B.S. Girgis, A.N.A. El-Hendawy, Porosity development in activated carbons

487   obtained from date pits under chemical activation with phosphoric acid,

488   Microporous and Mesoporous Materials 52 (2002) 105-117.

489   [38] M.C. Macias-Perez, M.A. Lillo-Rodenas, A. Bueno-Lopez, C.S.M. de Lecea, A.

490   Linares-Solano, SO2 retention on CaO/activated carbon sorbents. Part II: Effect of

491   the activated carbon support, Fuel 87 (2008) 2544-2550.

492   [39] J.L. Figueiredo, M.F.R. Pereira, M.M.A. Freitas, J.J.M. Orfao, Modification of the

493   surface chemistry of activated carbons, Carbon 37 (1999) 1379-1389.

494   [40] A. Martínez de Yuso, Development of activated carbons from lignocellulosic

495   wastes for toluene and h-hexane adsorption and recovery, University of San Jorge,

496   Spain, 2012.

497　　[41] J.S. Noh, J.A. Schwarz, Estimation of the point of zero charge of simple oxides by

498　　　　　mass titration, Journal of Colloid and Interface Science 130 (1989) 157-164.

499　　[42] J.A. Menendez, M.J. Illangomez, C. Leon, L.R. Radovic, On the difference

500　　　　　between the isoelectric point and the point of zero charge of carbons, Carbon 33

501　　　　　(1995) 1655-1657.

502　　[43] A.A.M. Daifullah, B.S. Girgis, Impact of surface characteristics of activated carbon

503　　　　　on adsorption of BTEX, Colloids and Surfaces a-Physicochemical and

504　　　　　Engineering Aspects 214 (2003) 181-193.

505　　[44] M.M. Dubinin, FUndamentals of the theory of adsorption in micropores of carbon

506　　　　　adsorbents - Characteristics of their adsorption properties and microporous

507　　　　　structures, Carbon 27 (1989) 457-467.

508　　[45] J.B. Castro, P.R. Bonelli, E.G. Cerrella, A.L. Cukierman, Phosphoric acid

509　　　　　activation of agricultural residues and bagasse from sugar cane: Influence of the

510　　　　　experimental conditions on adsorption characteristics of activated carbons,

511　　　　　Industrial & Engineering Chemistry Research 39 (2000) 4166-4172.

512　　[46] B.S. Girgis, S.S. Yunis, A.M. Soliman, Characteristics of activated carbon from

513　　　　　peanut hulls in relation to conditions of preparation, Materials Letters 57 (2002)

514　　　　　164-172.

515　　[47] C.A. Toles, W.E. Marshall, M.M. Johns, L.H. Wartelle, A. McAloon, Acid-

516　　　　　activated carbons from almond shells: physical, chemical and adsorptive

517　　　　　properties and estimated cost of production, Bioresource Technology 71 (2000).

518　　[48] M. MolinaSabio, F. RodriguezReinoso, F. Caturla, M.J. Selles, Development of

519　　　　　porosity in combined phosphoric acid carbon dioxide activation, Carbon 34

520　　　　　(1996) 457-462.

521   [49] D. Ramirez, S.Y. Qi, M.J. Rood, Equilibrium and heat of adsorption for organic

522   vapors and activated carbons, Environmental Science & Technology 39 (2005)

523   5864-5871.

524   [50] J. Pei, J.S. Zhang, Determination of adsorption isotherm and diffusion coefficient

525   of toluene on activated carbon at low concentrations, Building and Environment

526   48 (2012).

527   [51] W.S. Bouhamra, C.G.J. Baker, A.S. Elkilani, A.A. Alkandari, A.A.A. Al-Mansour,

528   Adsorption of toluene and 1,1,1-trichloroethane on selected adsorbents under a

529   range of ambient conditions, Adsorption-Journal of the International Adsorption

530   Society 15 (2009) 461-475.

531   [52] J. Benkhedda, J.N. Jaubert, D. Barth, L. Perrin, Experimental and modeled results

532   describing the adsorption of toluene onto activated carbon, Journal of Chemical

533   and Engineering Data 45 (2000) 650-653.

534   [53] Y.C. Chiang, P.C. Chiang, E.E. Chang, Effects of surface characteristics of

535   activated carbons on VOC adsorption, Journal of Environmental Engineering-

536   Asce 127 (2001) 54-62.

537   [54] I. Langmuir, The adsorption of gases on plane surfaces of glass, mica and

538   platinum, Journal of the American Chemical Society 40 (1918) 1361-1403.

539   [55] H. Marsh, B. Rand, Characterization of microporous carbons by means of Dubinin-

540   Radushkevich equation, Journal of Colloid and Interface Science 33 (1970).

541

542

Table 1. Preparation conditions of the activated carbons and labelling of samples.

Sample	Temperature (ºC)	IR[1]	Time (min)	Atmosphere
AT400R1t75	400	1	75	N_2
AT400R15t30	400	1.5	30	N_2
AT467R117T45	467	1.17	45	N_2
AT533R083t60	533	0.83	60	N_2
AT600R1t30	600	1	30	N_2
AT400R1t75-ox	400	1	75	$8\%O_2/N_2$
AT400R15t30-ox	400	1.5	30	$8\%O_2/N_2$
AT467R117T45-ox	467	1.17	45	$8\%O_2/N_2$
AT533R083t60-ox	533	0.83	60	$8\%O_2/N_2$
AT600R1t30-ox	600	1	30	$8\%O_2/N_2$

[1] Impregnation ratio: amount phosphoric acid (g) / amount almond shell (g)

Table 2. Ultimate analysis of activated carbons (% in dry basis).

Sample	C	H	N	S	O[1]	Yield[2]
AT400R1t75	75.20	2.42	0.31	n	22.07	68.4
AT400R15t30	72.40	3.13	0.49	n	23.98	69.2
AT467R117t45	70.00	2.72	0.30	n	26.98	70.6
AT533R083t60	68.70	2.12	0.38	n	28.80	72.9
AT600R1t30	68.47	2.05	0.42	n	29.06	73.2
AT400R1t75-ox	61.91	1.84	0.54	n	35.71	80.9
AT400R15t30-ox	60.35	3.31	0.45	n	35.89	83.0
AT467R117t45-ox	75.08	2.01	0.43	n	22.48	66.7
AT533R083t60-ox	69.56	2.16	0.44	n	27.84	72.0
AT600R1t30-ox	72.25	1.40	0.43	n	25.92	69.3

[1] By difference

[2] Mass of activated carbon/mass of precursor x 100

n: neligible

Table 3. Total amount of CO and CO_2 evolved up to 1100ºC in TPD experiments and pH_{PZC}.

Sample	CO (mmol/g)	CO_2 (mmol/g)	pH_{PZC}
AT400R05t120	2,17	1,32	4,04±0,39
AT400R15t30	1,80	0,75	4,54±0,10
AT467R117t45	2,18	1,18	3,39±0,14
AT533R083t60	2,23	0,39	2,36±0,11
AT600R1t30	3,04	0,45	1,89±0,05
AT400R1t75-ox	9,68	0,66	2,19±0,03
AT400R15t30-ox	1,43	0,60	2,07±0,02
AT467R117t45-ox	7,76	0,54	2,04±0,02
AT533R083t60-ox	9,54	0,61	1,74±0,01
AT600R1t30-ox	3,38	0,46	1,69±0,02

Table 4. Results from N_2 physisorption.

Sample	S_{BET} (m^2/g)	V_{meso}[1] (cm^3/g)	V_{micro}[2] (cm^3/g)	V_p (p/p$_0$ =0,995) (cm^3/g)	Microposity[3] (%)
AT400R1t75	1128±50	0,385	0,259	0,67	77,8
AT400R15t30	789±34	0,268	0,176	0,482	71
AT467R117t45	1117±44	0,494	0,181	0,724	70,9
AT533R083t60	891±36	0,341	0,194	0,571	74,6
AT600R1t30	926±37	0,375	0,182	0,624	69,7
AT400R1t75-ox	1408±57	0,334	0,112	0,899	69,2
AT400R15t30-ox	1198±51	0,525	0,185	0,900	70,3
AT467R117t45-ox	1277±51	0,490	0,161	0,894	74,9
AT533R083t60-ox	980±38	0,253	0,052	0,633	83,3
AT600R1t30-ox	1122±50	0,400	0,103	0,759	77,4

1 BJH method

2 t-plot method

3 According to Lillo-Rodenas et al., 2005

Table 5. Maximum adsorption capacity for toluene (mmol/g).

Sample	Experimental (mmol/g)	Langmuir model	
		Wm (mmol/g)	K (cm^3/g)
AT400R1t75	6,612	6,540	1,21
AT400R15t30	7,156	7,436	0,48
AT467R117t45	6,924	6,891	0,94
AT533R083t60	4,954	4,949	1,51
AT600R1t30	6,471	6,504	0,8
AT400R1t75-ox	6,372	6,310	0,74
AT400R15t30-ox	5,983	5,717	1,04
AT467R117t45-ox	6,825	6,691	0,86
AT533R083t60-ox	5,960	5,804	1,10
AT600R1t30-ox	5,759	5,628	1,25

FIGURE CAPTIONS

Figure 1. DTG curves for decomposition of low temperature activated carbons.

Figure 2. Results from Boehm titration.

Figure 3. Nitrogen adsorption isotherms.

Figure 4. Toluene adsorption isotherms.

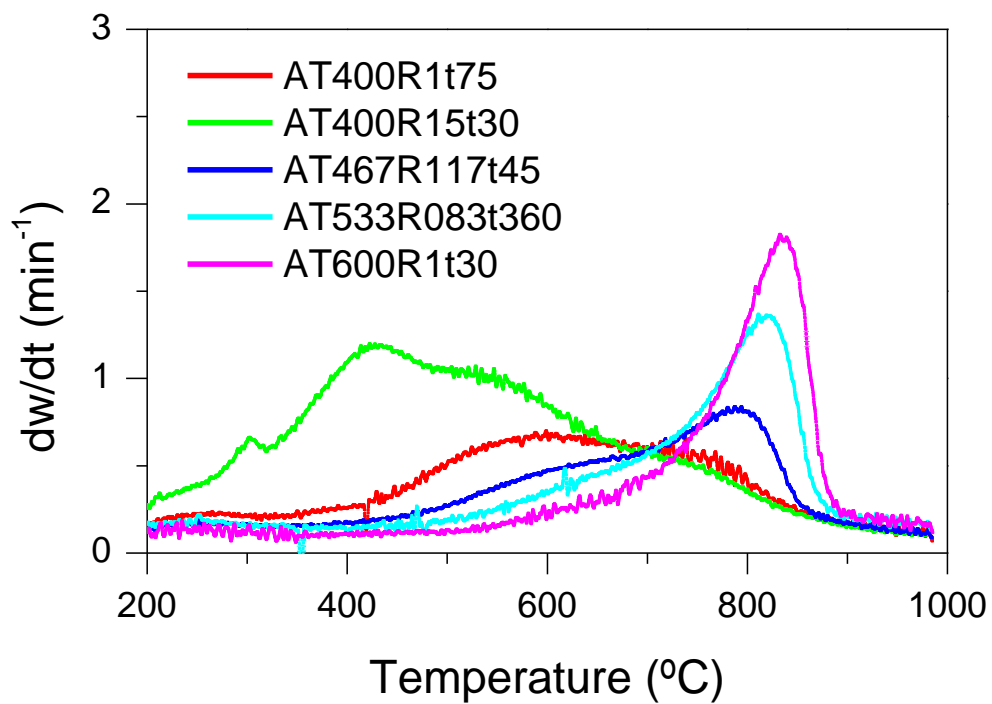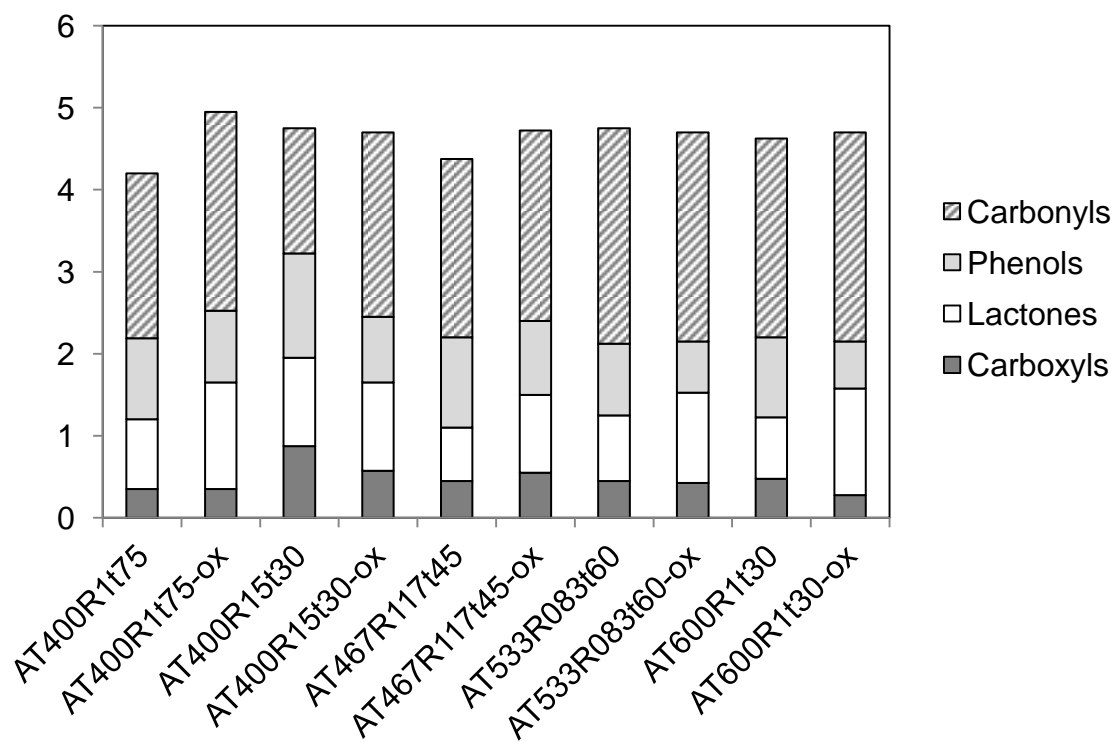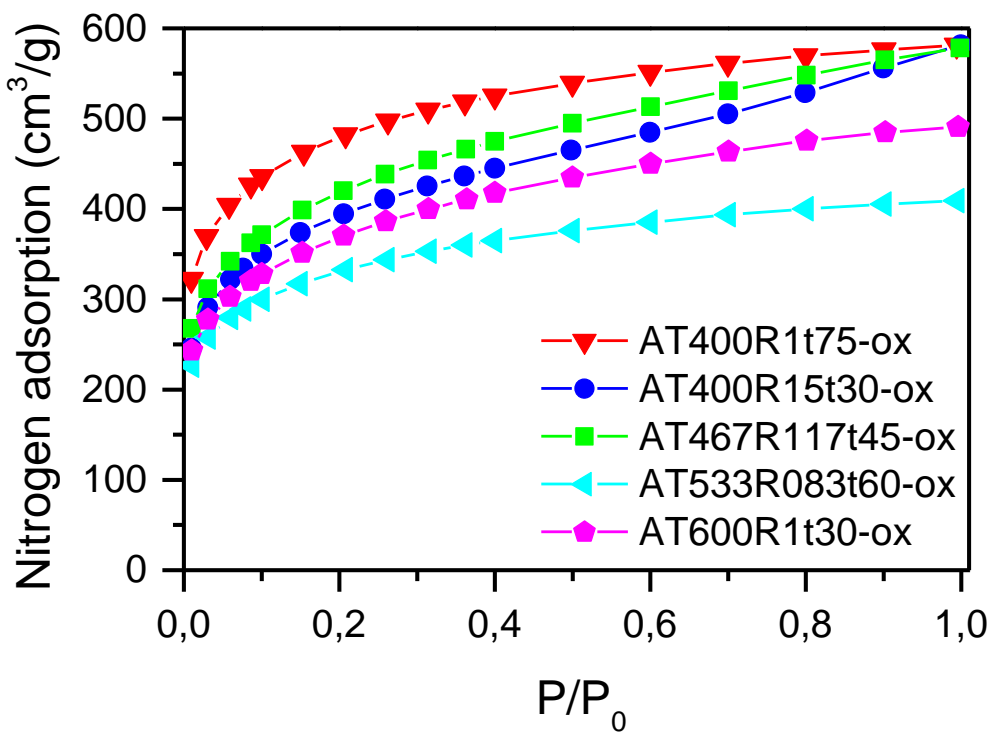**Figure 5.** Amount of toluene adsorbed as a function of the D-R slope at low $\log^2 p_0/p$.

Figure 1
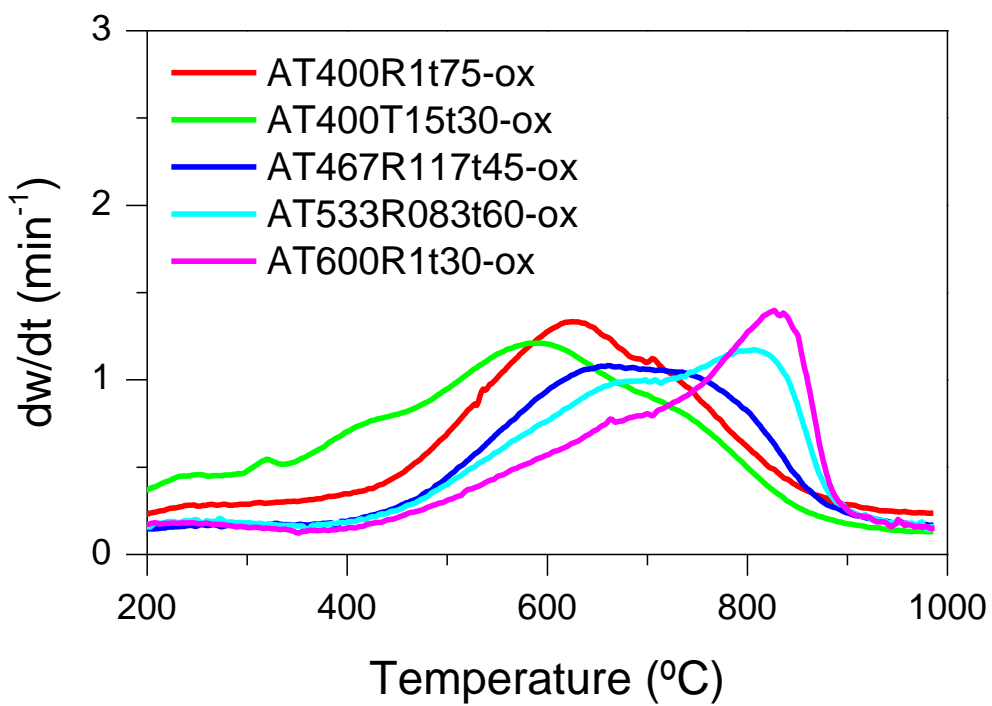
Figure 2

Figure 3

Figure 4

Figure 5